

TESTING SUSTAINABLE NICKEL ALLOYS MADE FROM RECYCLED SCRAP IN A SCO₂ ENVIRONMENT

^{1,2}Tereza VÁLKOVÁ, ¹Lucia ROZUMOVÁ, ¹Tomáš MELICHAR

¹Research Centre Řež, s.r.o., Husinec-Řež, Czech Republic, EU, <u>tereza.valkova@cvrez.cz</u> ²University of Chemistry and Technology Prague, Technická 1905, Prague, Czech Republic, EU

https://doi.org/10.37904/metal.2025.5143

Abstract

Metallic materials have made possible technological developments over thousands of years. The increased demand for structural nickel alloys in critical areas such as energy, construction, and safety are expected to drive production growth rates of up to 200 percent in 30 years. However, most of these materials take a significant amount of energy to extract and manufacture, and these processes create substantial volumes of greenhouse gases and pollutants. This study was done with the aim of enhancing nickel alloy reuse and examining recycled materials in the corrosion environment of supercritical carbon dioxide. The tested materials were Ni-base alloys Inconel 738 and Inconel 713. The recycled content of the newly created alloy was 50 percent and 100 percent. These specimens were then exposed to 1000 hours of loop operation at a maximum operating temperature of 550 °C and a maximum operating pressure of 25 MPa, with a constant flow rate of sCO₂ medium of 0.1 kg/s. The specimen surface, corrosion layer thickness and composition were evaluated by Scanning Electron Microscope (SEM) with Energy Dispersive Spectroscopy (EDS).

Keywords: Nickel alloys, sCO₂, sustainability, recycling, corrosion

1. INTRODUCTION

Nickel plays a crucial role in the transition to clean energy; however, its extraction and processing pose significant environmental and social challenges. Nearly half of the world's nickel is currently supplied by Indonesia, the largest nickel producer, which has seen fast expansion in output. However, this surge has resulted in community dislocation, air pollution, and deforestation. The nation's carbon footprint is further increased by its reliance on coal for nickel processing. Nickel has fluctuated in price. Due to a surplus of supply brought on by Indonesia's production boom, prices dropped from \$50,000 per tonne in 2022 to about \$16,400 per tonne in early 2024 [1]. Long-term demand is anticipated to increase despite this decline, driven by the electric car industry's preference for nickel-rich batteries due to their higher energy density and range. Stainless steels and superalloys, which account for up to 65% of production, are another key application for nickel in industry and energy. These days, the question is: can we guarantee a steady supply of nickel? Governments and industries are increasingly focusing on responsible sourcing and environmental regulations to ensure nickel remains a sustainable pillar of the clean energy revolution [2 - 4].

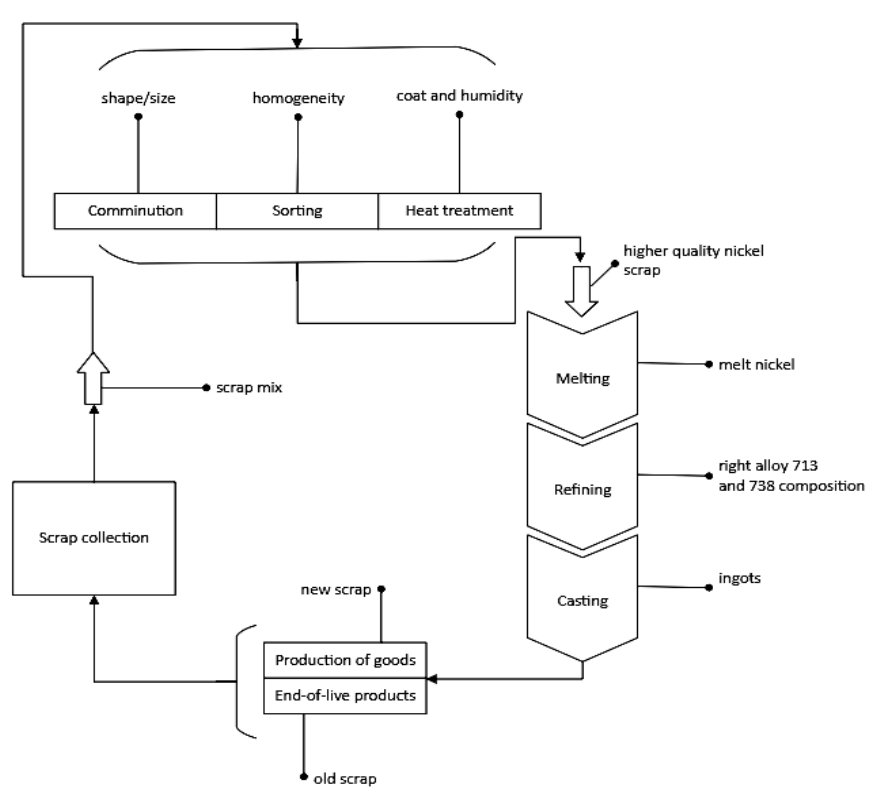
One of the options for greater sustainability of nickel is its recycling. Nickel alloys are metal combinations in which nickel is the primary element, typically mixed with other metals such as chromium, iron, copper, or molybdenum. In this study, we focus on Inconel, where the main components of the alloy are nickel and chromium. Inconels are known for their ability to withstand harsh environments, making them ideal for applications that require high-performance materials. The unique properties of these alloys make them indispensable in industries where durability and resistance to heat, oxidation, and corrosion are critical. Recycled nickel alloys are typically cheaper to produce than new alloys made from raw materials. The cost savings are passed on to industries, making recycled materials an attractive alternative for manufacturers [5].



Consequently, we took the decision to test corrosion alloys manufactured from recyclable materials. Inconel is by nature significantly more costly than stainless steel, which is frequently utilized in supercritical CO2 applications. But in this case, the price is competitive. An excellent sustainable material would be alloys that are less expensive and more resistant against corrosion than stainless steel. The Ni-base alloys Inconel 738 and Inconel 713 were the materials that were subjected to the test.

2. PREPARATION AND MELTING OF SCRAP IN NICKEL ALLOYS RECYCLING

Recycling nickel alloys is a well-established process that involves several stages (**Figure 1**). The general flow includes collection, sorting, cleaning, degreasing, processing with size reduction, and remelting to produce high-quality recycled alloys [6, 7]. Numerous businesses throughout the world focus on recycling nickel alloys, contributing significantly to the circular economy by reusing valuable metals from sectors including manufacturing, oil and gas, and aerospace. Here are a few well-known players: PCC Revert Group (Caledonian Alloys and Greenville Metals), Globe Metal, Revert International, Monico Alloys and well-known Greystone Alloys [8, 9].



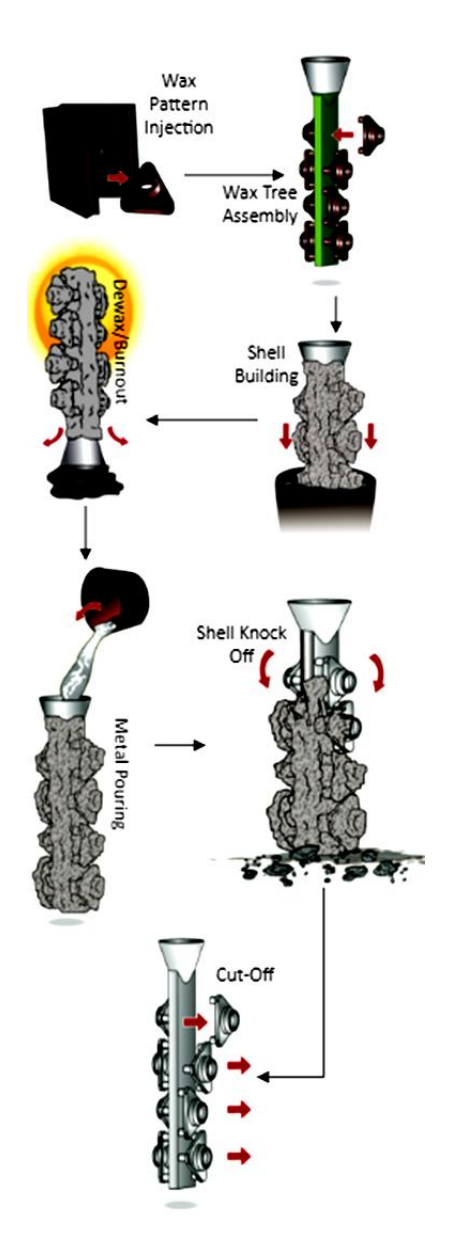


Figure 2 The investment casting process [11]

Figure 1 Flow chart of secondary Ni refining operations

In Czech Republic, the recycling of nickel alloys has long been the focus of the Prague-based company Walter Praguecast, from whom we obtained materials for testing. These alloys were created from leftover material from the manufacturing of precision heat-resistant castings, which are essential components of gas turbines' stator and rotor stages. Investment Casting Technology was the process utilized to create the castings [10]. Investment casting involves several stages that ensure precision and minimal material waste (**Figure 2**). A



wax or polymer pattern is made, replicating the shape of the final component. Then patterns are assembled onto a tree-like structure and coated with ceramic slurry to form a shell. The mold is heated, and the wax is melted and drained, leaving a hollow ceramic shell. After that molten metal, in this case, recycled Inconel 713 and Inconel 738, is poured into the shell. Once solidified, the shell is broken off, and the casting is cleaned and machined as required [12]. The ability of investment casting to produce complex shapes with tight tolerances makes it an excellent fit for high-performance materials like Inconels.

2.1 Corrosion behavior of nickel alloys in sCO₂

Due to Inconel alloys naturally resist corrosion at high temperatures, they are often well suited for supercritical CO₂ (sCO₂) conditions. For long-term stability in modern energy systems, however, oxidation, carburization, and other degradation mechanisms must be minimized by careful consideration of particular alloy selection and operating circumstances. According to the corrosion mechanism, ion diffusion primarily regulates the corrosion process of materials in sCO₂, which is further subdivided into oxidation and carburization (comprehensive article on corrosion mechanism by Yang.). Because nickel-based alloys may create a strong oxide layer to stop further corrosion, they are more corrosion resistant than ferritic/martensitic steel and austenitic stainless steel. Furthermore, the nickel matrix exhibits a reduced solubility and diffusivity of C as well as a lower activity of Cr. The corrosion of alloys in sCO₂ is often accelerated by the presence of impurities such O₂, H₂O, CO, and SO₂. The oxidation process will be accelerated by the addition of CO and O₂ (with H₂O). Corrosion will worsen, spallation will happen, and the produced oxide layer will thicken [13, 14].

Inconel, a widely used alloy, is characterized by its properties tailored for specific conditions. Inconel 625, a highly resistant alloy, forms a stable chromium oxide layer when exposed to high temperatures, slowing down corrosion. However, prolonged exposure can lead to internal oxidation and microstructural degradation, impacting its long-term performance. Inconel 718, on the other hand, is suited for high-pressure, moderate temperature sCO₂ conditions, withstanding temperatures up to approximately 650°C. Its strength lies in its ability to form chromium-rich oxide layers, offering excellent oxidation resistance. However, long-term exposure can result in microstructural changes, compromising its mechanical strength, making it primarily suitable for applications with moderate thermal demands. Because of the production of Fe-oxide or Cr-oxide rich scales on their surface, chromatia-forming alloys 625 and In718 demonstrated superior corrosion resistance compared to FB2 and 17-4-PH. This outcome was mostly ascribed to alloys 62 and In718 having greater Cr contents (article by Rozumova). It was shown that the Cr concentration mostly determined how well steels and alloys corroded in supercritical carbon dioxide [15, 16]. Alloys 690 and 600, which are nickel-base alloys that generate chromia, depend on the chromia layer to shield them from oxygen damage in hightemperature CO₂ [17]. Furthermore, certain Mn-Cr spinel oxides were produced on the surface of the chromia layer in nickel-base alloys as a result of the fast diffusion of Mn in the chromia layer. It has been observed that the consumption of Cr was slowed down by the slower growth of the Mn-Cr spinel oxides compared to the single Cr [18].

3. EXPERIMENTAL SET-UP AND MATERIALS

An experimental loop at CVR was used to examine the corrosion of metals in supercritical carbon dioxide conditions; it was commissioned in 2017. The loop was intended to operate at a maximum temperature of 550 °C, a maximum working pressure of 25 MPa in the high-pressure portion, and a maximum pressure of 12.5 MPa in the low-pressure section, with a flow rate of 0.4 kg/s. The loop was filled with carbon dioxide from a pressure vessel with a purity of 4.5 (99.995% by volume) [19].

3.1 Conditions

Specimens were exposed to 1000 hours of loop operation at a maximum operating temperature of 550 °C and a maximum operating pressure of 25 MPa, with a constant flow rate of sCO₂ medium of 0.1 kg/s. More details



about sCO₂ loop at CVR are in article from Rozumová [15].

3.2 Materials

From the castings, corrosion coupons were made by cutting into in the shape of a prism with dimensions of 10 x 40 x 2 mm. The coupons were sanded with 4000 grit sandpaper. **Table 1** shows the alloy composition based on data given by the manufacturer.

Table 1 The list of tested materials with chemical composition (wt%)

	Element (wt %)									
Alloy	С	Ni	Cr	Мо	Ti	W	Co	Nb	Αl	Fe
Inconel 713	0,03	Bal.	11	3,8	0,5	-	1	2,5	5,5	0,5
Inconel 738	0,11	Bal.	16	2	3,7	2,6	9	0,9	3,4	0,3

One set of Inconel 713 specimens was produced using a composition of 50% recycled material and 50% new alloy. Another set of Inconel 713 specimens was manufactured entirely from recycled material (100% recycled content). A batch of Inconel 738 specimens was prepared with a mixture comprising 50% recycled material and 50% fresh alloy. Another batch of Inconel 738 specimens was fabricated exclusively from recycled material, utilizing 100% recycled content.

4. RESULTS AND DISCUSSION

4.1 Weight gains

First, changes (or rather increases) were determined the weight of the specimens after exposure and recalculated per unit area of the specimen. Changes in the weight of the specimens are usually proportional to the corrosion damage of the specimens after exposure. The results are summarized in the graph in **Figure 3**.

Inconel 738 exhibited significantly higher weight gains compared to Inconel 713. A surprising outcome was the lower weight gain observed in materials produced entirely from 100% recycled content compared to those containing a 50% addition of recycled material.

The weight gains correspond to the thickness of the corrosion layers on the surface of the exposed materials. For Inconel 738, the average thickness of the oxide layer was 0,38 μ m, whereas for Inconel 713, the average oxide layer thickness was 0.20 μ m (**Figure 4**).

0.0006 0.0005 0.0004 0.0003 0.0002 0.0001 0.00001 0.00001 0.00001 0.00001 0.00001 0.00001 0.00001 0.00001 0.00001 0.00001 0.00001 0.00001 0.00001 0.00001 0.00001 0.00001 0.00001 0.00001 0.00001 0.00001 0.00001 0.00001 0.00001 0.00001 0.00001 0.00001 0.00001 0.00001 0.00001 0.00001 0.00001 0.00001 0.00001 0.00001 0.00001 0.00001 0.00001 0.00001 0.00001 0.00001 0.00001 0.00001 0.00001 0.00001 0.00001 0.00001 0.00001 0.00001 0.00001 0.00001 0.00001 0.00001 0.00001 0.00001 0.00001 0.00001 0.00001 0.00001 0.00001 0.00001 0.00001 0.00001 0.00001 0.00001 0.00001 0.00001 0.00001 0.00001 0.00001 0.00001 0.00001 0.00001 0.00001 0.00001 0.00001 0.00001 0.00001 0.00001 0.00001 0.00001 0.00001 0.00001 0.00001 0.00001 0.00001 0.00001 0.00001 0.00001 0.00001 0.00001 0.00001 0.00001 0.00001 0.00001 0.00001 0.00001 0.00001 0.00001 0.00001 0.00001 0.00001 0.00001 0.00001 0.00001 0.00001 0.00001 0.00001 0.00001 0.00001 0.00001 0.00001 0.00001 0.00001 0.00001 0.00001 0.00001 0.00001 0.00001 0.00001 0.00001 0.00001 0.00001 0.00001 0.00001 0.00001 0.00001 0.00001 0.00001 0.00001 0.00001 0.00001 0.00001 0.00001 0.00001 0.00001 0.00001 0.00001 0.00001 0.00001 0.00001 0.00001 0.00001 0.00001 0.00001 0.00001 0.00001 0.00001 0.00001 0.00001 0.00001 0.00001 0.00001 0.00001 0.00001 0.00001 0.00001 0.00001 0.00001 0.00001 0.00001 0.00001 0.00001 0.00001 0.00001 0.00001 0.00001 0.00001 0.00001 0.00001 0.00001 0.00001 0.00001 0.00001 0.00001 0.00001 0.00001 0.00001 0.00001 0.00001 0.00001 0.00001 0.00001 0.00001 0.00001 0.00001 0.00001 0.00001 0.00001 0.00001 0.00001 0.00001 0.00001 0.00001 0.00001 0.00001 0.00001 0.00001 0.00001 0.00001 0.00001 0.00001 0.00001 0.00001 0.00001 0.00001 0.00001 0.00001 0.00001 0.00001 0.00001 0.00001 0.00001 0.00001 0.00001 0.00001 0.00001 0.00001 0.00001 0.00001 0.00001 0.00001 0.00001 0.00001 0.00001 0.00001 0.00001 0.00001 0.00001 0.00001 0.00001 0.00001 0.00001 0.00001 0.00001 0.00001 0.00001 0.00001 0.00001 0.00001 0.00001 0.00001 0.00001 0.00001 0.00001 0.00001 0.00001 0.00001 0.00001 0.00001 0.00001 0.00

Figure 3 Mass changes (mg.cm⁻²) of specimens of Inconel 738 (orange color) and Inconel 713 (green color) after exposure in sCO₂ at 550 °C for 1000 hours

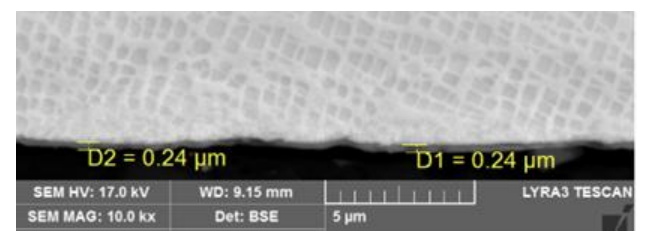


Figure 4 SEM image of Inconel 713 (with a 50 % addition of recycled material) showing the measurement of the corrosion layer thickness

4.2 Characterization of the corrosion layers

After exposure, the specimens were cut metallographically,

ground using 1200-grit sandpaper, and polished with diamond paste (3 μ m and 1 μ m). Light optical microscopy (LOM) was used for surface morphology analysis. LOM allows for the examination of surface features of materials, such as pits, cracks, and general corrosion patterns. This helps in identifying the type of corrosion.



However, LOM has limitations in terms of resolution, and it may require complementary techniques (e.g., SEM, EDS, or XRD) for detailed chemical or crystallographic analysis. An oxide layer was then examined, and its thickness was measured using a Scanning Electron Microscope (SEM, LYRA3 TESCAN), equipped with Backscatter Electron (BSE) imaging and Energy Dispersive Spectroscopy (EDS) for chemical composition analysis.

Glow Discharge Optical Emission Spectrometry (GD-OES) was also employed for elemental analysis, similar to SEM-EDS, but with the additional capability to quantify carbon content in each layer of the specimen. This method provides insights into specimen carbonation, which can cause structural damage and accelerate corrosion. Elemental analysis was conducted using the Horiba JobinYvon GD Profiler 2 atomic emission spectrometer. The XRD analysis was performed using PANalytical X'Pert PRO + High Score Plus. IN **Figures** 5 to 8 are documented results of LOM and SEM analyses of Inconel 738 and Inconel 713 with an addition of recycled material.

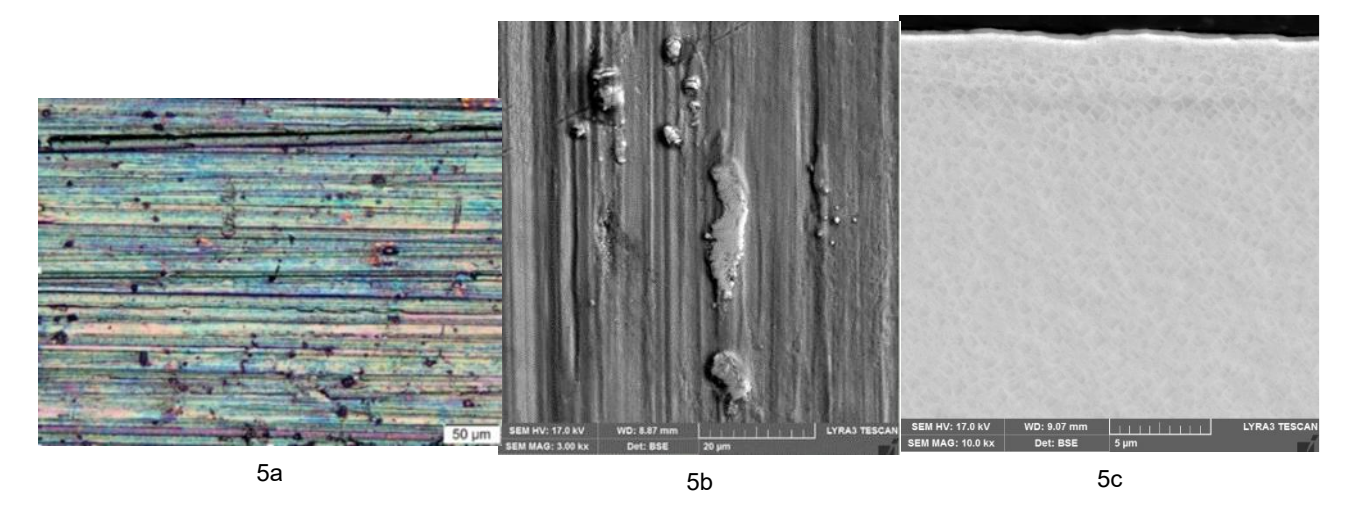
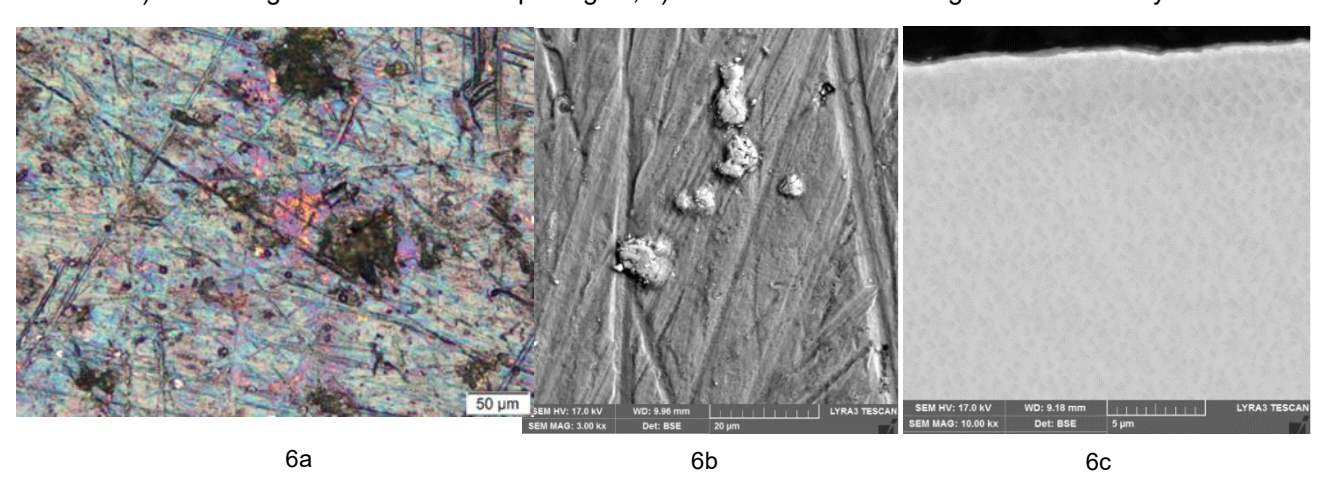


Figure 5 Inconel 738 with a 50% addition of recycled material: a) LOM image of the surface morphologies; b) SEM image of the surface morphologies; c) cross section SEM image of corrosion layer





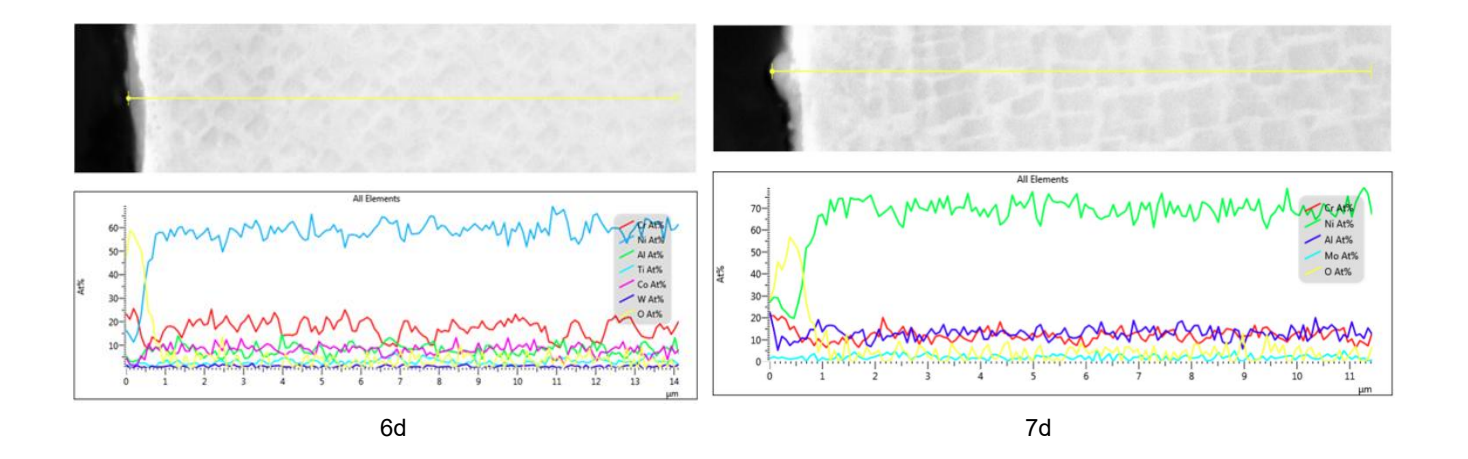


Figure 6 Inconel 738 with a 100% recycled content: a) LOM image of the surface morphologies; b) SEM image of the surface morphologies; c) cross section SEM image of corrosion layer; d) EDS linescan of the oxide layer

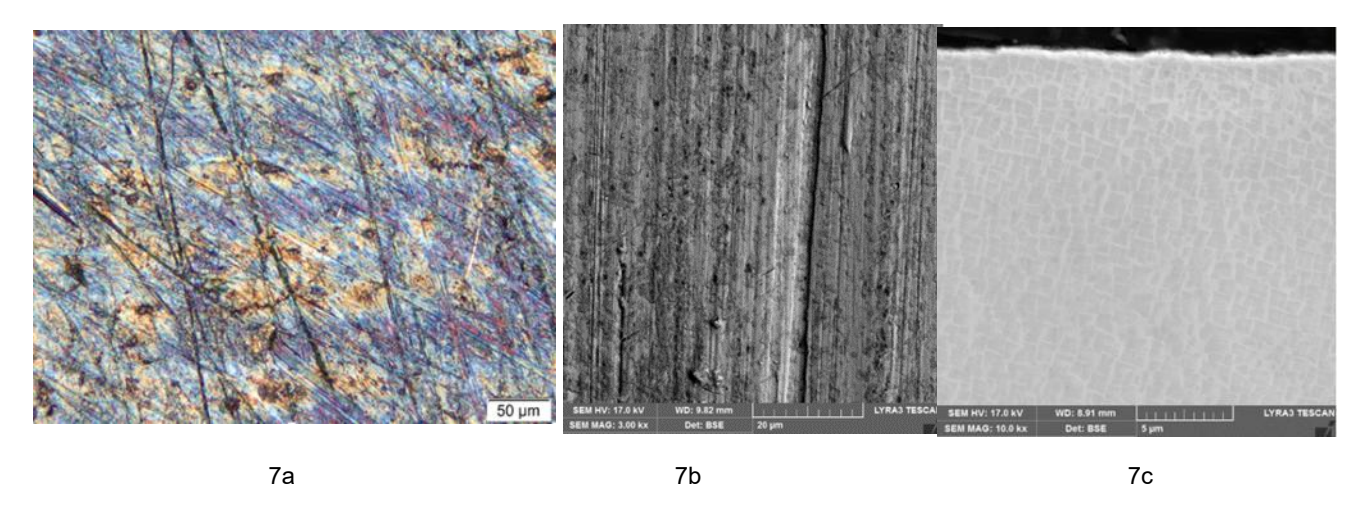


Figure 7 Inconel 713 with a 50% addition of recycled material: a) LOM image of the surface morphologies; b) SEM image of the surface morphologies; c) cross section SEM image of corrosion layer; d) EDS linescan of the oxide layer

After 1000 hours of exposure to supercritical CO₂, a compact protective oxide layer formed on the surfaces of Inconel 713 and Inconel 738. In the case of Inconel 738, the surface layer consisted of oxygen, chromium, and nickel (**Figure 6d**). For Inconel 713, the protective layer was composed of oxygen, chromium, nickel, and additionally aluminum (**Figure 7d**). In both alloys, no internal oxidation was observed; only external oxidation was present. Carbonization of the materials is not evident from **images 5c, 6c, 7c**, and **8c**. Furthermore, carbonization was not confirmed by GDOES analysis, as demonstrated in **Figure 9**.

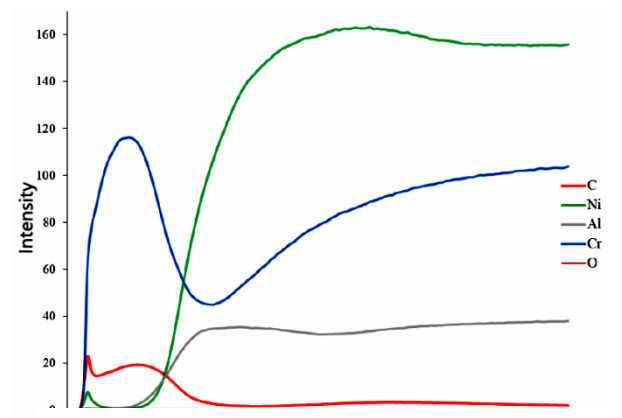


Figure 9 Graph of GD-OES analysis of In738 with a 100% recycled content



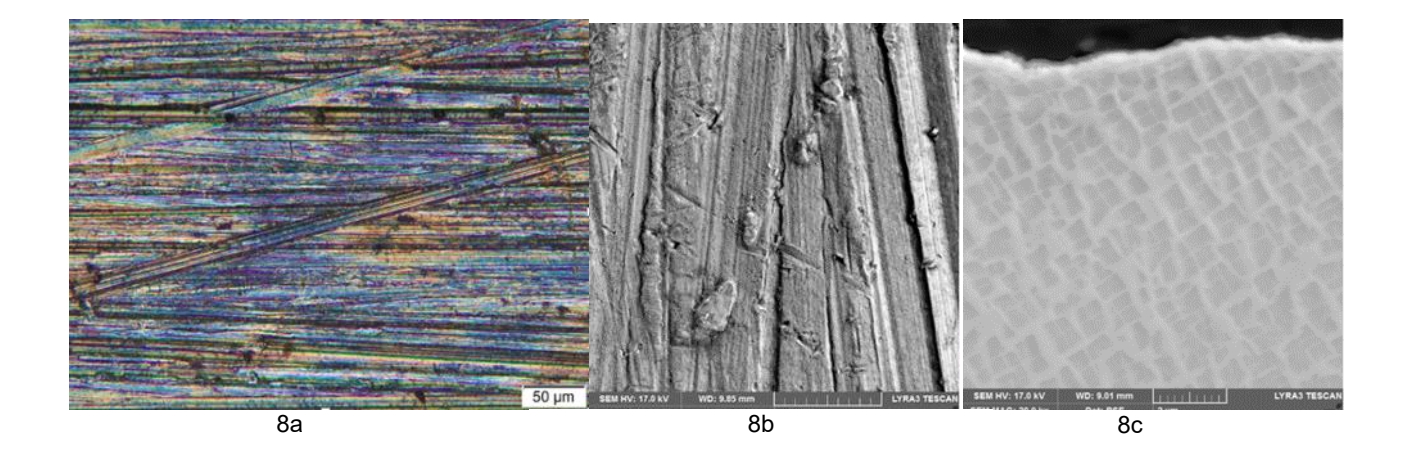


Figure 8 Inconel 713 with a 100% recycled content: a) LOM image of the surface morphologies; b) SEM image of the surface morphologies; c) cross section SEM image of corrosion layer

The XRD results of surface analyses provided crucial confirmation of the observations made through SEM-EDS analyses of the surfaces. While SEM-EDS offered valuable insights into the elemental composition and distribution across the surface layers, XRD complemented these findings by identifying the crystalline phases present. This combination of techniques allowed for a more comprehensive understanding of the surface characteristics.

During the cross-sectional analyses, impurities or large particles were repeatedly observed. In the case of **Figure 10**, niobium particle was identified, which contribute to increased corrosion attack and accelerate material degradation. A higher number of impurities were detected in specimens with a 100% recycled material fraction.

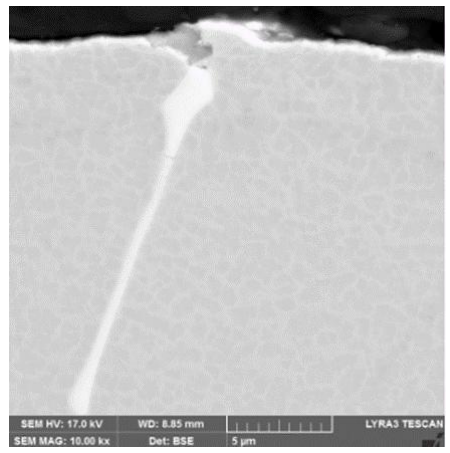


Figure 10 The SEM-BSE image of the 738 alloy with a 100% recycled material fraction shows the presence of niobium particle

5. CONCLUSION

The oxidation resistance of Inconel alloys in supercritical CO_2 environments is paramount, as corrosion from supercritical CO_2 and its impurities can significantly degrade material performance. Inconel 738 and Inconel 713 are known for their excellent oxidation resistance, primarily due to the formation of a protective chromium oxide (Cr_2O_3) scale on their surface. However, this behavior can be altered by the presence of impurities or variations in alloy composition, which can occur in recycled materials. Key benefits of recycling nickel alloys are resource conservation, lower environmental impact, cost efficiency and energy savings. However, there are several challenges associated with recycling high-performance alloys like Inconel:

- **Contamination:** During recycling, impurities can be introduced, which may alter the alloy's composition. These contaminants could degrade the alloy's properties, including its oxidation resistance, creep strength, and fatigue performance.
- **Segregation:** The melting and re-solidification process can result in segregation of alloying elements, which can lead to inhomogeneous microstructures and compromised material properties. For example, the distribution of critical elements like aluminum, titanium, or molybdenum may become uneven in recycled alloys, affecting the alloy's performance in high-stress applications.
- Recrystallization and Grain Growth: Repeated heating and cooling cycles during recycling may lead



to recrystallization or abnormal grain growth, which can negatively impact the mechanical properties of the alloy, particularly at high temperatures.

Loss of Alloying Elements: Some alloying elements, such as niobium, tantalum, and zirconium, may
volatilize or be lost during recycling, which can affect the superalloy's strength, oxidation resistance, and
overall performance.

Despite these challenges, when managed carefully, recycled Inconel alloys can retain much of their desirable properties and perform similarly to their virgin counterparts. The ability to produce high-quality recycled alloys depends on the control of the recycling process, the purity of the scrap material, and the proper adjustment of alloying elements.

ACKNOWLEDGEMENTS

The presented work was financially supported by the Czech Science Foundation Project No.TK02030023 "The coolant purification technology for supercritical CO2 circuits." co-financed from the state budget by the Technology Agency of Czech Republic (TA CR) under the Theta Programme.

At CVR, the presented work has been realized with Institutional Support from the Ministry of Industry and Trade of the Czech Republic. The presented results were obtained using the CICRR infrastructure, which is financially supported by the Ministry of Education, Youth and Sports - project LM2023041.

REFERENCES

- [1] CASEY, J. Rystad Energy: Nickel demand to outstrip supply by 2024. *Global Mining Review*. 2021, October 13. https://www.globalminingreview.com/special-reports/13102021/rystad-energy-nickel-demand-to-outstrip-supply-by-2024/.
- [2] CHANDLER, David L. 3 Questions: Can we secure a sustainable supply of nickel? *MIT News Publication*. 2024, November 1, Massachusetts Institute of Technology. https://news.mit.edu/2024/3-questions-can-we-secure-sustainable-supply-nickel-1101.
- [3] NOLAN, S. Nickel: Driving the future of EV battery technology globally. *EV Magazine*. 2024, October 25. https://evmagazine.com/technology/nickel-driving-the-future-of-ev-battery-technology-globally.
- [4] ARLTOVÁ, M. Mine more and more sustainably. Electric car manufacturers need nickel, battery recycling will help them in 25 years. 2022, May 5. Euro.cz. https://www.euro.cz/clanky/tezit-vice-a-udrzitelneji-vyrobci-elektromobilu-potrebuji-nikl-recyklace-baterii-jim-pomuze-az-za-25-let/.
- [5] *Nickel recycling*. (n.d.). Nickel Institute. Retrieved October 20, 2024, https://nickelinstitute.org/en/policy/nickel-life-cycle-management/nickel-recycling/.
- [6] ESTRADA, I. *Nickel alloy. Greystone alloys scrap metal recycling*. ISO 9001 certified. 2024, September 26. https://www.greystonealloys.com/metals/nickel-scrap-recycling/.
- [7] CAPUZZI, S., TIMELLI, G. Preparation and melting of scrap in aluminum recycling: A review. *Metals*. 2018, vol. 8, p. 249. https://doi.org/10.3390/met8040249.
- [8] KOLLOVÁ, A., PAUEROVÁ, K. Superalloys characterization, usage and recycling. *Manufacturing Technology*. 2022, vol. 22, no. 5, pp. 550–557. https://doi.org/10.21062/mft.2022.070.
- [9] Alloys & Metals Greystone alloys scrap metal recycling. 2024, October 8 ISO 9001 certified. https://www.greystonealloys.com/alloys-we-recycle/.
- [10] Walter Praguecast products and services. Walter Praguecast. 2020. https://www.praguecast.cz/products-and-services.
- [11] What is Investment Casting?. Investment Casting Institute. 2023. https://www.investmentcasting.org/what-is-investment-casting.html.



- [12] HORÁČEK, M. Dimensional accuracy of castings produced by the investment casting process, Thesis, VUT, 2009. https://dspace.vut.cz/items/15b31dd1-c888-4e38-ad28-e20e30ac3f57.
- [13] YANG, L., QIAN, H., KUANG, W. Corrosion behaviors of heat-resisting alloys in high temperature carbon dioxide. *Materials*. 2022, vol. 15, no. 4, p. 1331. https://doi.org/10.3390/ma15041331.
- [14] KANG, Y., LENG, X., ZHAO, L., BAI, B., WANG, X., CHEN, H. Review on the corrosion behaviour of nickel-based alloys in supercritical carbon dioxide under high temperature and pressure. *Crystals.* 2023, vol.13, no. 5, p. 725. https://doi.org/10.3390/cryst13050725.
- [15] ROZUMOVÁ, L., MELICHAR, T., VELEBIL, L. Microstructural evaluation of preselected steels for turbine after supercritical CO₂ exposure. 2021, pp. 98–105. https://doi.org/10.17185/duepublico/73951.
- [16] Gui, Y., Liang, Z., Shao, H., Zhao, Q. Corrosion behavior and lifetime prediction of VM12, Sanicro 25 and Inconel 617 in supercritical carbon dioxide at 600 °C. *Corrosion Science*. 2020, vol. 175, p. 108870.
- [17] LEE, H.J., SUBRAMANIAN, G.O., KIM, S.H., JANG, C. Effect of pressure on the corrosion and carburization behavior of chromia-forming heat-resistant alloys in high-temperature carbon dioxide environments. *Corrosion Science*. 2016, vol. 111, pp. 649–658.
- [18] NGUYEN, T.D., ZHANG, J., YOUNG, D.J. Effects of Si, Al and Ti on corrosion of Ni-20Cr and Ni-30Cr alloys in Ar-20CO₂ at 700 °C. *Corrosion Science*. 2018, vol. 130, pp. 161–176.
- [19] BALLEK, J. Carbon dioxide power cycles. UCT Prague Institutional Repository [online]. 2019. https://repozitar.vscht.cz/theses/31093/.